## University of Bristol - Explore Bristol Research
### General rights

CrossMark

# Aligned discontinuous intermingled reclaimed/virgin carbon fibre composites for high performance and pseudo-ductile behaviour in interlaminated carbon-glass hybrids

Marco L. Longana[*], HaNa Yu, Meisam Jalavand, Michael R. Wisnom, Kevin D. Potter

*ACCIS, University of Bristol, Bristol, BS8 1TR, UK*

ABSTRACT

Highly aligned intermingled fibre composites are produced from reclaimed and virgin carbon fibres using the High Performance Discontinuous Fibre (HiPerDiF) method. The stiffness and strength characteristics of these materials are studied as a function of the reclaimed to virgin fibres ratio. Interlaminated hybrid composites with discontinuous carbon fibre preforms sandwiched between continuous glass fibres are designed to demonstrate pseudo-ductility and allow investigation of the effect of the mixing ratio of reclaimed and virgin carbon fibres on the nonlinear stress-strain curve shape. The pseudo-ductile behaviour is explained by adapting the Damage Mode Map to describe the failure process of inter-laminated hybrid specimens with different low elongation material strength. It is concluded that the HiPerDiF method is a valuable platform to remanufacture reclaimed carbon fibres into a high perfor-mance and potentially economical value recycled composite material. The Damage Mode Maps can be used to optimise the pseudo-ductile response of the interlaminated hybrid material.

## 1. Introduction

The wide spread of carbon fibres reinforced polymers (CFRPs) in various engineering and industrial sectors over the last decades poses the challenge of dealing with production waste and end-of life products, particularly if we consider that carbon fibres pre-serve high intrinsic value. The simple disposal in landfill or incin-eration are increasingly discouraged by the legislation. The mechanical comminution of CFRP and the dispersion of the chop-ped fibres as fillers in replacement for glass fibres limit the deriv-able value. In order to apply the circular economy model to composite materials, recycling processes that will allow reclaiming the fibres with minimal loss of mechanical properties and rema-nufacturing them into high performance materials need to be developed and integrated. A complete review about the technolo-gies to recycle CFRPs for structural applications was presented by Pimenta and Pinho [1]. Amongst the fibre reclamation processes it is worth mentioning pyrolysis, i.e. thermochemical decomposition of the matrix at elevated temperatures in an inert environment [2], oxidation in a fluidised bed, i.e. the matrix elimination at high

temperature in oxygen-rich flow [3], chemical recycling in various reactive media at moderate temperature, e.g. catalytic solutions [4], benzyl alcohol [5], or at higher temperature and pressure in su-percritical fluids [6–9].

Of greater interest for the presented work is, independently from the fibre recovery process, the remanufacturing of the reclaimed fibres into CFRP and their mechanical response. When the reclamation process preserves the reinforcement architecture of the waste the reclaimed fibres can be used as it is [10]. However, the size-reduction of CFRP waste before reclamation, the fibre breakage during reclamation and the chopping of the fibres after reclamation lead to fibres that are fragmented to short lengths. As a result, the only industrially relevant remanufacturing processes for reclaimed fibres so far are direct moulding techniques, e.g. injection moulding [11] and bulk moulding compound compression [12], and the compression moulding of intermediate random [13] or aligned mats [14]. However, to deliver improved recycled materials, a high fibre alignment is the key factor to increase the fibre volume frac-tion, and consequently the performances of recycled composites [15,16]. Various techniques, already used for the alignment of short fibres, have been taken in consideration for the remanufacturing of reclaimed carbon fibres. A modified papermaking technique was applied to reclaimed fibres from the University of Nottingham

* Corresponding author.
 *E-mail address:* m.l.longana@bristol.ac.uk (M.L. Longana).

research group [14,17,18] reaching 80% of the theoretical alignment value and a fibre volume fraction of 45% with a moulding pressure of 100 bar. Wong et al. [19] proposed the use of a centrifugal alignment rig, which uses a dispersion of fibres in a viscous media accelerated through a convergent nozzle installed in a rotating drum, as remanufacturing technique for reclaimed carbon fibres. An alignment level of 90% was obtained using 5 mm fibres. The same authors [19] worked on a hydrodynamic spinning process of a viscous fibre suspension. Janney et al. [20] developed the Three Dimensional Engineered Preform Process (3-DEP) adding multiple motions control to a pulp moulding process tool and therefore the control of fibre areal weight and orientation.

The HiPerDiF method, developed at the University of Bristol [21], has proven to be an effective way to manufacture composite materials with high levels of alignment from discontinuous fibres. This unique fibre orientation mechanism uses the momentum change of a water-fibre suspension to align the fibres. It was previously noted that tensile modulus, strength and failure strain of aligned discontinuous fibre composites produced with the HiPerDiF method were close to those of continuous fibre composites provided that the fibres are accurately aligned and their length is sufficiently long compared to the critical fibre length [22,23]. The use of the HiPerDiF method allows the production of high performance recycled carbon fibre composites from reclaimed discontinuous carbon fibres. Therefore, this method enables the efficient recovery of value from end-of-life components and production wastes, and is well placed in the developing of a supply and processing chain of recycled carbon fibre composites and in a circular economy model, as demonstrated also by Ref. [25].

As described in Ref. [22] the HiPerDiF method can be used to produce hybrid composites with different configurations, these allowed obtaining pseudo-ductile behaviour from glass-carbon and carbon-carbon intermingled composite [23,24], this can be further tailored if intermingled composites are coupled with continuous glass fibres to generate interlaminated composites [24].

The present work is aimed at evaluating the effect of reclaimed fibres on the mechanical properties of intermingled and interlaminated hybrid composites. In a first stage, the performances of intermingled reclaimed and virgin carbon discontinuous fibre (rCF and vCF respectively) composites are assessed. A good knowledge about the mechanical properties of combined reclaimed/virgin carbon fibre composite will help to maximise the use of reclaimed carbon fibres taking account the related economic advantages. Subsequently, plies of intermingled discontinuous fibres, with different ratios of rCF/vCF, are interlayered in continuous glass/epoxy prepreg layers to study the effect on tensile behaviour of carbon/glass hybrid composites.

## 2. The HiPerDiF method

The HiPerDiF method is a novel technique that allows aligning discontinuous fibres [21,22]. The technique was originally developed to study the behaviour of aligned discontinuous fibre composites as a function of fibre type, length and alignment level within the HiPerDuCT (High Performance Ductile Composite Technology) project [23]. The working principle exploits the sudden momentum change of a jet of fibres suspended in water directed in a narrow gap between parallel plates as shown in Fig. 1.

In the HiPerDiF process, the fibres are dispersed in a liquid medium (water) that is accelerated through a nozzle to partially align the fibres. The fibre suspension jet is directed to the orientation head, which is comprised of parallel plates with a controllable gap. The fibres are aligned transversely to the suspension jet by a sudden momentum change of the liquid, provided that the gap is a maximum of 1/3 the fibre length. Subsequently, the fibres fall

on a perforated conveyor belt that is running parallel to the narrow gap direction; a suction plate, placed underneath the belt, removes the water maintaining the fibre orientation. The aligned fibre preform is then dried with infrared radiations to allow the resin impregnation process. This method allowed obtaining highly-aligned and high fibre volume fraction discontinuous CFRPs: for composites with a 41% fibre volume fraction ($v_f$), 65% of fibres were in the range of $\pm 3°$ to perfect alignment, and in the case of composite specimens with 55% of $v_f$, 67% of fibres were in the range of $\pm 3°$ to perfect alignment [22]. Moreover, using high strength fibres (Young's Modulus 225 GPa, Strength 4350 MPa), mechanical properties comparable to those of continuous fibres were achieved: a Young's Modulus of 80.6 GPa and a strength of 816 MPa for 41% of $v_f$ and a Young's Modulus of 115 GPa and a strength of 1509 MPa for 55% of $v_f$ [22]. In addition, the HiPerDiF method enabled intimately mixing two or more different fibre types in one preform due to its intrinsic manufacturing capabilities [23,24].

One of the exceptional potentials of HiPerDiF technology is that it makes it possible to achieve high mechanical properties and a high value by remanufacturing reclaimed carbon fibres into highly-aligned, high-performances unidirectional composites [24]. These preforms have also the potential to achieve pseudo-ductile behaviour. To do so, two approaches are considered in this paper: (i) intermingled rCF/vCF composites and (ii) interlaminated hybrid composites with an embedded layer of intermingled rCF/vCF sandwiched between continuous glass fibre layers.

## 3. Experiment

### 3.1. Materials

High tensile strength virgin carbon fibres (C124, TohoTENAX, [26]) and reclaimed carbon fibres (AS4, Hexcel) from a M56 resin composite with the pyrolysis "cycle B" process defined by Pimenta and Pinho in Ref. [27] were used. The mechanical properties are summarised in Table 1.

The intermingled preforms with rCF/vCF are coupled with a MTM49-3 epoxy resin film [28] and partially impregnated by applying a pressure of 30 bar at a temperature of 60 °C. The mechanical properties of the continuous E- and S-glass composite layers used for the interlaminated hybrid specimens, measured with tensile tests conducted with the specimens shown in Fig. 2, are summarised in Table 2. Please note that these glass/epoxy composites were manufactured in a closed mould and therefore the fibre volume fraction was about 15% higher than one obtained with specimens manufactured on an open tool-plate. For the interlaminated hybrid composites, the rCF/vCF preform was impregnated during the curing process by the resin excess from the continuous glass fibre prepreg.

### 3.2. Specimen preparation

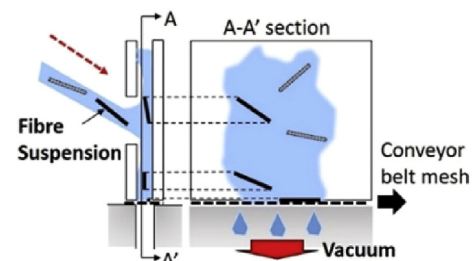The specimens were prepared by vacuum bag moulding. The



**Fig. 1.** HiPerDiF fibre alignment mechanism, front view and cross-section (A-A') [22].

intermingled fibre composites were cured in an autoclave for 135 min at a temperature of 135 °C and a pressure of 6 bar. The interlaminated composites were cured according to the curing cycle of the continuous glass prepreg, i.e. 90 min at a temperature of 125 °C and a pressure of 6 bar. Burrs at all edges of cured samples were gently removed. GFRP end-tabs were bonded with Huntsmann Araldite 2014-1 adhesive. A schematic of the specimen is shown in Fig. 2. The nominal thickness of the intermingled rCF/vCF composites, manufactured with four plies of discontinuous carbon fibres, is 0.22 mm. The nominal thickness of the interlaminated glass/carbon composites, manufactured with the stacking sequence [ContG$_2$/DiscC$_2$/ContG$_2$], where ContG represents a continuous glass layers and DiscC an aligned discontinuous carbon fibre preforms, is 0.50 mm for the ones with E-glass and 0.56 mm for the ones with S-glass. A view of the cross-section is shown in Fig. 2.

### 3.3. Test method

Tensile tests were performed on an electro-mechanical testing machine with a cross-head displacement speed of 1 mm/min. The load was measured with a 10 kN load cell (Shimadzu, Japan) and the strain was measured with a video extensometer (Imetrum, UK). A white speckle pattern over a black background was spray painted on the specimens to allow the strain measurement with the video extensometer. The gauge length for the strain measurement was slightly less than 50 mm.

### 3.4. Intermingled rCF/vCF composites fibre volume fraction calculation

To be able to better interpret the stiffness and strength data of the interlaminated specimens, it is necessary to measure the fibre volume fraction (Vf). The estimation of the Vf through image analysis of microscopy images of the cross-section was deemed unreliable as it is affected by the fibre misalignment and dependent on the arbitrary grey threshold value chosen to distinguish fibre and matrix. In a first attempt, the resin burn-off method, codified in the ASTMD3171 standard, was used. This proved to be unreliable as the discontinuous fibres were blown away by the internal air circulation in the furnace. Considering the low weight of each specimen, even the loss of a small amount of fibre during the resin burn-off compromises the fibre volume fraction measurement. It was therefore decided to estimate a nominal fibre volume fraction Vf$_{Nom}$ with Equation (1) based on the measured initial stiffness:

$$Vf_{Nom} = \frac{E_{Mes}}{\eta \left( Q_{fR} E_R + Q_{fV} E_V \right)} \tag{1}$$

where Q$_f$ is the fibre fraction, E is the modulus of the fibres, the subscript R and V refer to reclaimed and virgin fibre, while E$_{Mes}$ is the measured modulus of the intermingled fibre composite. As in

**Table 1**
Fibres mechanical properties.

| Fibre properties | Virgin fibres[a] | Reclaimed fibres[b] |
|---|---|---|
| Fibre type, Manufacturer | C124, TohoTENAX | AS4, Hexcel |
| Diameter [μm] | 7 | 6.5 |
| Length [mm] | 3 | 3 |
| Density [g/cm$^3$] | 1.82 | 1.79 |
| E$_{11}$ [GPa] | 225 | 230 |
| Failure σ$_{11}$ [MPa] | 4350 | 1110 |
| Failure ε$_{11}$ [%] | 1.9 | 0.5 |

[a] From manufacturer data sheet [26].
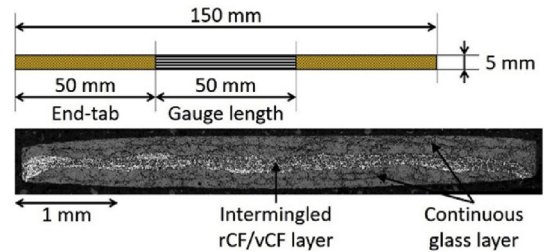[b] Measured with single fibre tests, a gauge length of 10 mm [27].



**Fig. 2.** Specimen geometry: top view and cross-section of interlaminated specimen.

Ref. [22], the discontinuity and misalignment of the fibres are taken into account by the factor η. Considering that the alignment level is independent of the nature of the fibre and both virgin and reclaimed fibre have the same length, the factor η is assumed to be the same for all virgin-reclaimed fibre combinations. A value of 0.85 was chosen with considerations similar to those discussed by Yu et al. in Ref. [22].

## 4. Results and discussion

### 4.1. Intermingled rCF/vCF composites

Batches of 3 specimens with 100% virgin and reclaimed fibres as well as blends with 10%, 20%, 25%, 30%, 40%, 50%, 60% and 80% of reclaimed fibres by volume were manufactured and tested. The measured tensile modulus as a function of the reclaimed fibre content in the composite is summarised in Fig. 3a. The stiffness of the rCF/vCF composite materials is fairly independent of the content of reclaimed fibres. The average stiffness is 71.2 GPa and the coefficient of variation is 7.6% based on all of the specimens with different ratios of rCF/vCF. The relatively high coefficient of variation can be explained considering that a coefficient of variation of 7.7% around an average fibre volume fraction of 36% was observed. Furthermore, variations in the fibre volume fraction are reflected in slight variations of the fibre alignment level. The modulus of the specimens remanufactured with 100% reclaimed fibres is 71.8 GPa and the coefficient of variation is 2.2%, to the authors' best knowledge this is amongst the highest values of remanufactured recycled composites with 3 mm carbon fibres that can be found in the available literature.

The specimens showed linear-elastic behaviour with brittle failure. The measured tensile failure strain and strength as a function of the reclaimed fibre ratio in the composite are summarised in Fig. 3b. The failure strain and stress, even if affected by the stress concentration in proximity of the end-tabs where all the specimens failed, follow an approximately linearly reducing trend between 0% and 50% of reclaimed fibre, and are substantially constant at higher reclaimed fibre ratios. As expected, considering the different nature of the tests, the failure strain of the reclaimed fibre/epoxy composites, 0.84%, is higher than the failure strain measured in Ref. [27] on single reclaimed fibres, 0.5%. In particular, it has to be remembered that the reclaimed fibre length used to remanufacture the composite (3 mm) is lower than the one used to measure the fibre properties in Ref. [27] (10 mm): this reduces the occurrence of reclamation-generated defects able to cause fibre failure. Moreover the fibres come from end-of-life carbon 'fabric' composites: it is reasonable to hypothesize the unit size of fabric weaving pattern to be much smaller than the 10 mm gauge length of the single fibre test samples, this generates several weakness points caused by damage in weaving.

It is possible to estimate a failure envelope for the strength using the linear or the bilinear rule of mixtures (RoM) developed

**Table 2**
Continuous glass composite properties from tensile test.

| | $E_{11}$ [GPa] | Failure $\sigma_{11}$ [MPa] | Failure $\varepsilon_{11}$ [%] | Ply thickness [mm] |
|---|---|---|---|---|
| Hexcel E-Glass/913 | 53.5 | 1252 | 2.54 | 0.097 |
| Hexcel S-Glass/913 | 58.4 | 1886 | 3.73 | 0.112 |

for hybrid composites [29], as shown in Fig. 4. The intermingled rCF/vCF composite can be considered as a hybrid composite constituted by two types of fibres with the same stiffness since the stiffness difference between rCF and vCF is only 2.2% as shown in Table 1. However, a high difference can be observed in the failure strains so, in this case, the reclaimed fibres act as the low elongation and the virgin fibres as the high elongation constituent. In terms of strength, it is commonly accepted that the linear RoM represents the upper bound. While the lower bound is defined by a bilinear RoM. The bilinear RoM is defined by the combination of two construction line, the dotted lines in Fig. 4. The linearly decreasing construction line represents the contribution of the virgin fibres to the overall strength as a function of their amount in the material. The "horizontal" construction line represents the strength contribution of the reclaimed fibres. The strength for the bilinear RoM, at a given amount of reclaimed fibres, is represented by the higher strength value of the two construction lines.

To be able to draw the rule of mixture curves, the strength is normalised, using Equation (2), to a common fibre volume fraction ($Vf_{Com}$) value of 60%.
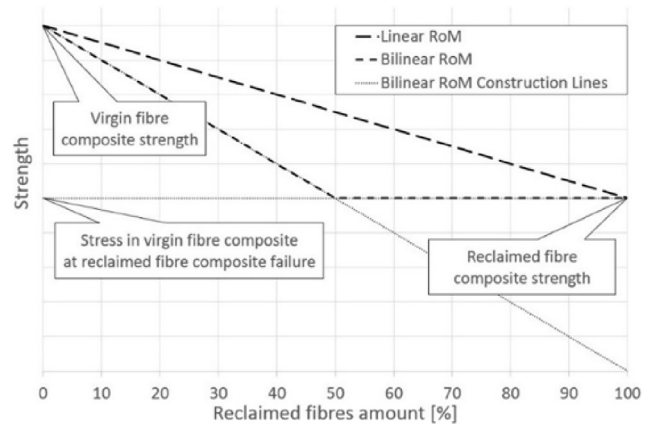


**Fig. 4.** Definition of linear and bilinear rule of mixtures, adapted from Ref. [30].

$$Normalised\ strength = \frac{Vf_{Com} \times Measured\ strength}{Vf_{Nom}} \qquad (2)$$

The nominal fibre volume fraction of the intermingled specimens ($Vf_{Nom}$) was estimated as described in Equation (1), Section 3.4, and it was found to vary between 42.5% and 32.4%.

The strength values of both the virgin and reclaimed fibre composites used as the input to the RoM of Fig. 5 are obtained from the tests results presented above. However, by observing Fig. 3b, it is clear that the failure values for the 0% rCF specimen are incongruous with the other data, i.e. are lower than the values obtained with 10% rCF and comparable with 20% and 25% rCF. This can be explained considering that the 0% rCF preforms, despite being able to generate high fibre volume fraction and high stiffness specimens, present a lower fibre alignment level attributable to mishandling during manufacturing. This renders the assumption in Section 3.4 not true and it is not possible to normalise the strength value for the 0% rCF specimens. These results are therefore discarded. To be able to use the RoM envelopes described in Fig. 4, the value of 0% rCF was estimated with a linear regression of the failure stress and strain values in the interval 10%–50% rCF. The normalised strength along with the estimated envelope is shown in Fig. 5a.

Because the composite stiffness as a function of the reclaimed fibre content is constant and the stress-strain curves show a linear elastic-brittle behaviour, the same construction described in Fig. 4 for the strength can be applied to the failure strain, as shown in Fig. 5b.

In Fig. 5, it can be observed that the strength and the failure strain are bounded by the RoM envelope and are closer to the bilinear rule of mixtures. In particular, they follow a diminishing trend, dominated by the virgin fibre properties up to 50% of reclaimed fibre content. Beyond this threshold, the values are substantially constant and correspond to the strength of the reclaimed fibre composite. It is possible to conclude that, in this case, quantity higher than 50% of virgin carbon fibres should be added to composite manufactured from reclaimed fibres to obtain an appreciable increase in the tensile strength and failure strain. However, it would be more efficient to increase the failure stress and strain values of the reclaimed fibre by increasing the lower strength boundary, i.e. the "horizontal" bilinear RoM construction line in Fig. 4, making the addition of virgin fibre not worthwhile at all.

### 4.2. Interlaminated continuous glass fibre and discontinuous rCF/vCF composites

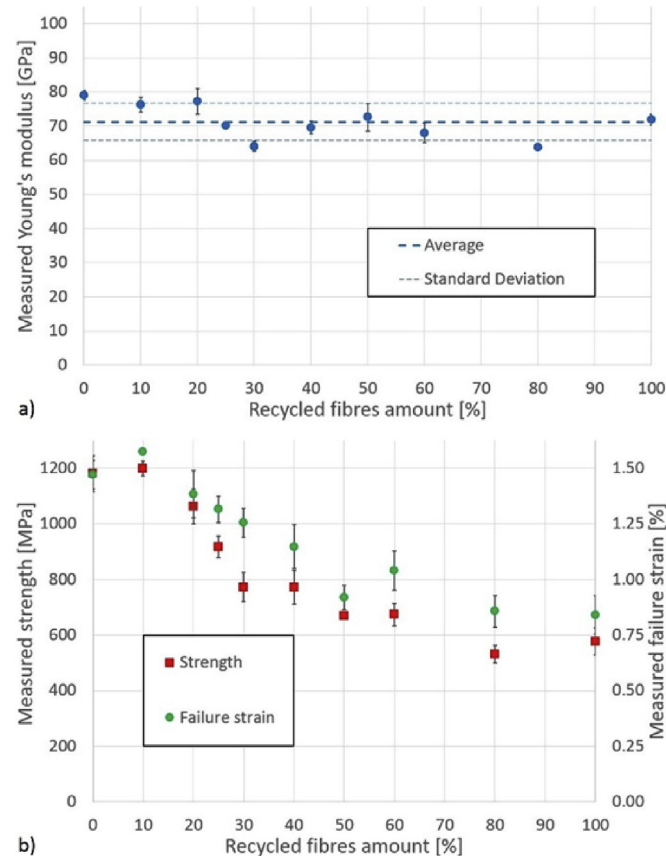The interlaminated specimens were manufactured by



**Fig. 3.** Measured mechanical properties of intermingled specimens as a function of the reclaimed fibre content: a) Stiffness; b) Failure stress and strain.
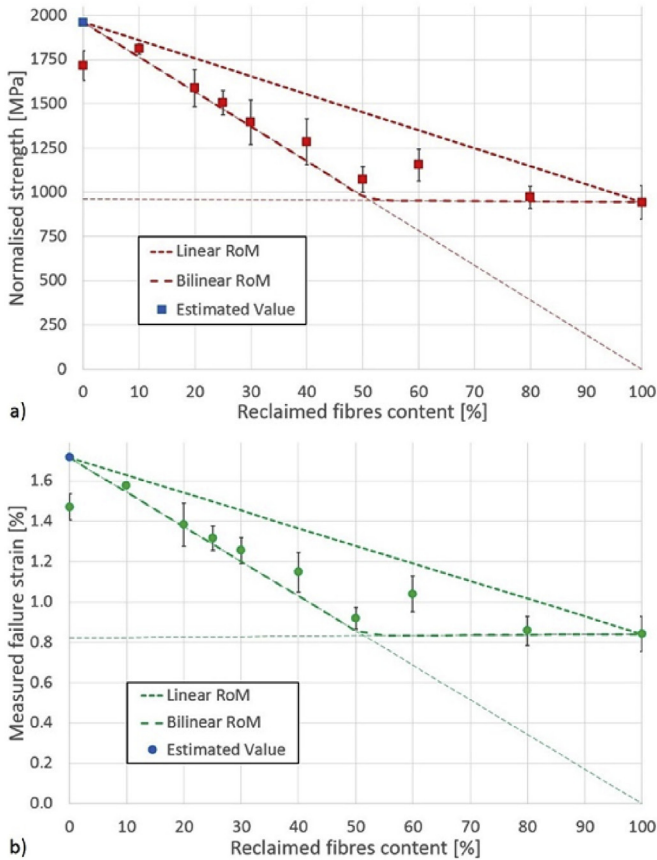
**Fig. 5.** Rule of Mixture application: a) Normalised strength as a function of the reclaimed fibre content in the composite; b) Measured failure strain as a function of the reclaimed fibre content in the composite.

S-glass has a higher stiffness and strength than E-glass, therefore interlaminated hybrids made with S-glass, shown in Fig. 6b, can withstand higher loads after the full fragmentation of the low strain material and can achieve higher elongations before failing. Of particular interest in Fig. 6b is the stress-strain curve for the 0% rCF (100% vCF) that presents a sharp change in slope, i.e. a reduction of tangent stiffness, due to onset of damage whereas the other curves show a smoother change. The case of 0% rCF (100% vCF) in Fig. 7b is similar to the case of 25% rCF of Fig. 7a: in this case, however, after the single delamination, the continuous S-glass is still able to carry the load. By increasing the content of rCF in the intermingled layers, and therefore reducing the strain at which the fragmentation starts, it can be observed that the density of the fragmentations in the carbon layer increases, as clearly shown in Fig. 7b and summarised below.

The initial $E_{11}$ of the two sets of specimens, as a function of the reclaimed fibre content, is shown in Fig. 8a. It can be observed that, as in Fig. 3a, the stiffness is independent of the rCF content. More interesting is to observe the dependence of the pseudo-yielding stress and strain on the rCF content, as shown in Fig. 8b. The pseudo-ductile properties of each case were measured based on the definition suggested by Wisnom et al. [31]. The pseudo-yield stress is defined by the intersection of the stress–strain curve and a straight line with the initial modulus $E_{11}$ and 0.1% offset from the origin, this definition is equivalent to the definition of proof stress in metals. The pseudo-yield strain is calculated with Hook's law using the initial modulus $E_{11}$ and the identified pseudo-yield stress.

The beginning of the low elongation material fragmentation is dictated by the rCF content. Moreover, as in Fig. 5, the onset of the
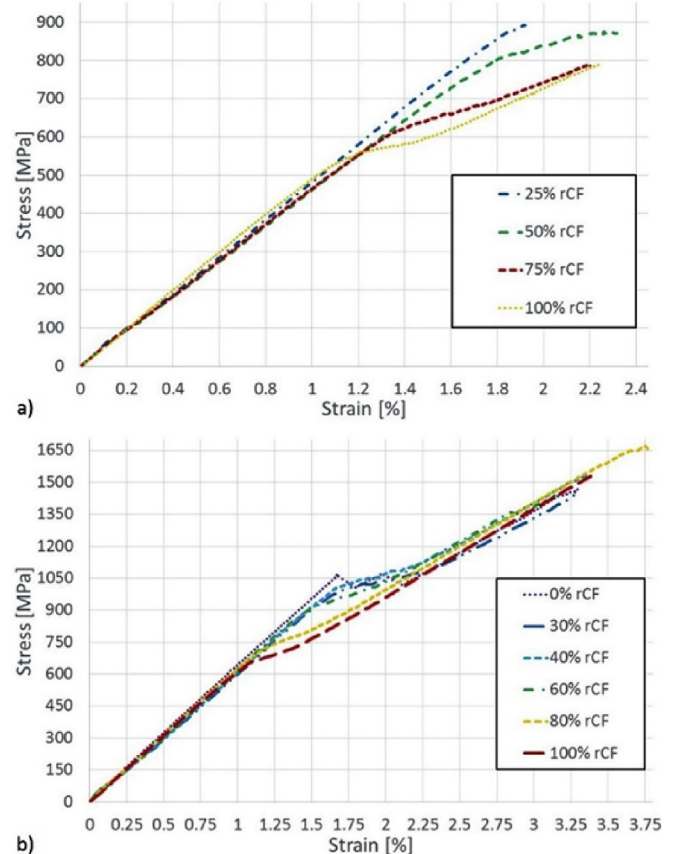
embedding two layers of dry intermingled rCF/vCF in the middle of four layers of continuous unidirectional glass fibre prepreg, as described above. Two sets of batches of 3 specimens were tested. One set was manufactured using E-glass and intermingled rCF/vCF preforms with ratio of 25%, 50% and 75% and rCF only. The other set was manufactured using S-glass and intermingled rCF/vCF preforms with ratio of 30%, 40%, 60% and 80% as well as rCF and vCF only.

Representative stress-strain curves for the interlaminated hybrid specimens with E-glass and S-glass are shown in Fig. 6. Fig. 7 shows typical tested interlaminated hybrid specimens with E-glass and S-glass and different rCF/vCF ratios, the total tensile strain applied is 2.5%.

For the interlaminated specimens with E-glass, Fig. 6a, the stress-strain curve of the 25% rCF content shows an almost linear-elastic behaviour up to failure and a brittle fracture. When the rCF content is increased, the tensile response becomes non-linear with knee points appearing when the low elongation material, i.e. the rCF-vCF inner layer, begins to fragment. A transition from brittle, i.e. failure of the glass layer (Fig. 7a, 25% rCF), to gradual failure, i.e. fragmentation of the carbon layer (Fig. 7a, 75% and 100% rCF), can be observed here. Of particular interest is that in the case of 50% rCF of Fig. 7a, both carbon layer fragmentation and glass fibre failure happen almost simultaneously.

The tensile response of the hybrid laminates made with S-glass is shown in Fig. 6b, a trend similar to E-glass can be observed: larger contents of reclaimed fibres led to earlier deviation from the initial linear elastic behaviour.



**Fig. 6.** Stress-strain curves of interlaminated hybrid composites with intermingled rCF/vCF: a) With E-glass; b) With S-glass.
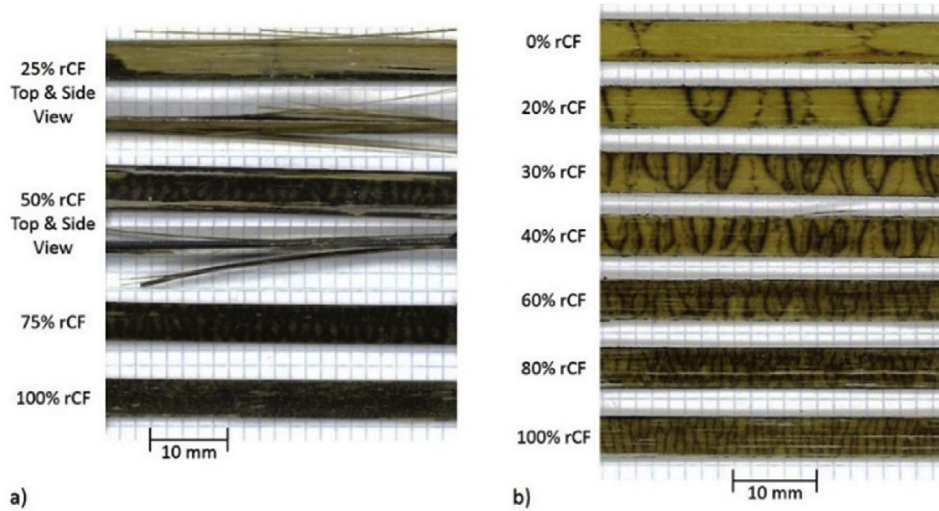
**Fig. 7.** Typical interlaminated hybrid samples after the tensile test, strain 2.5% circa: a) With E-glass; b) With S-glass.

fragmentation is driven by the vCF content. In the case of the E-glass interlaminated composites no fragmentation can be observed for rCF contents lower than 50% and the pseudo-yield stress and strain values decrease approximately linearly with the increase of the rCF content beyond 50%. Similarly, in the case of the S-glass the pseudo-yield values tend to remain constant up to rCF content of 50% and then decrease.

However, it is interesting to note that the pseudo-yield strain, i.e. the strain level at which the fragmentation process establishes itself with a significant number of fractures is higher than the failure strain identified in Fig. 3b, as shown in Fig. 9a. This can be explained considering the fact that the continuous high elongation fibres protect the low elongation fibres from the stress concentration at the end-tab region [32] coupled with the effect of a broader strength distribution in the intermingled rCF-vCF layer, as explained in Ref. [33]. The main mechanism for the hybrid effect was identified to be the altered failure development due to statistical effects on formation of clusters of fibre breaks. The high strength scatter in the carbon layer caused by mixing rCF and vCF can alter the failure development and delay the critical cluster formation and thereby increase the apparent failure strain of the rCF-vCF layer in the hybrid composite.

Moreover it is interesting to note that the fragmentation intervals, measured by dividing the gauge length by the number of fragments on the specimen surface, is reduced by the increase of the rCF content, i.e. by the carbon layer strength reductions, as shown in Fig. 9b. This implies that a higher number of fragments can be created by increasing the amount of rCF. It can be concluded that by changing the content of rCF in the intermingled fibre layer it is possible to tailor the tensile response of interlaminated hybrid composites. The stiffness is not affected by the rCF content but the nonlinear behaviour is different depending on the content of reclaimed carbon fibres. By controlling the rCF content it is possible to set the position of the pseudo-yielding point on the stress-strain curve; this allows tailoring of the nonlinear behaviour and defining the consequent pseudo-ductile strain.

Damage Mode Maps, proposed conceptually in Ref. [34] and further developed analytically in Refs. [35,36], are an efficient tool to understand the failure process of different hybrid specimens. These maps also can help to find optimal combinations based on the applied constraints. In the original Damage Mode Maps [34–36], all the material properties (including those of the low and high strain materials and the interface) were constant and the
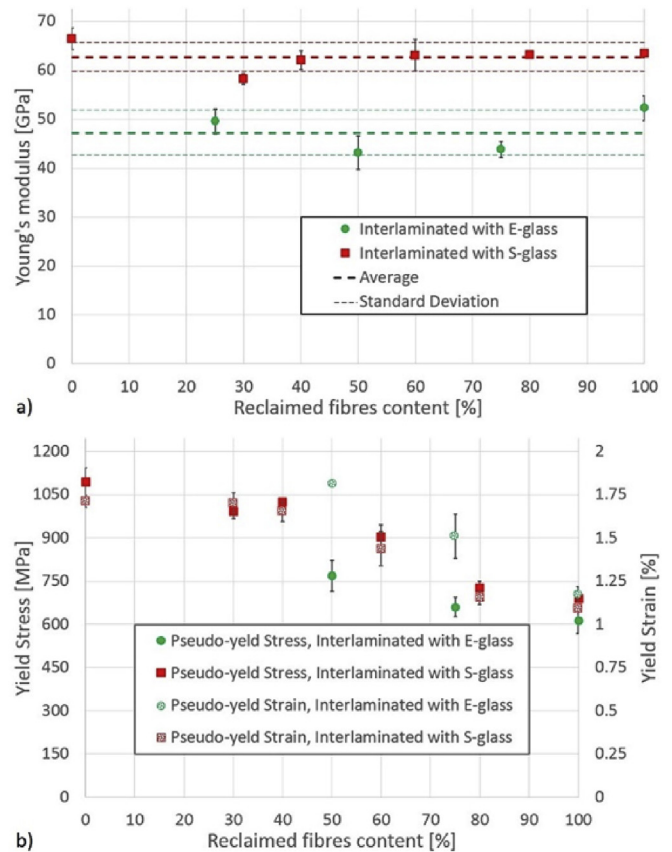


**Fig. 8.** Measured mechanical properties of interlaminated specimens as a function of the reclaimed fibre content: a) Stiffness; b) Failure stress and strain.

thickness of the low and high strain material were treated as the unknowns. However, in the present work, the failure strain of the low strain material (the intermingled rCF/vCF composite) varies with the ratio of reclaimed to virgin fibres and the previous representation of the Damage Mode Map concept was not suitable for this study. Therefore, a new type of Damage Mode Map has been developed with the failure strain of the low strain material, i.e. the carbon layer, on the horizontal axis to study the effects of the rCF/
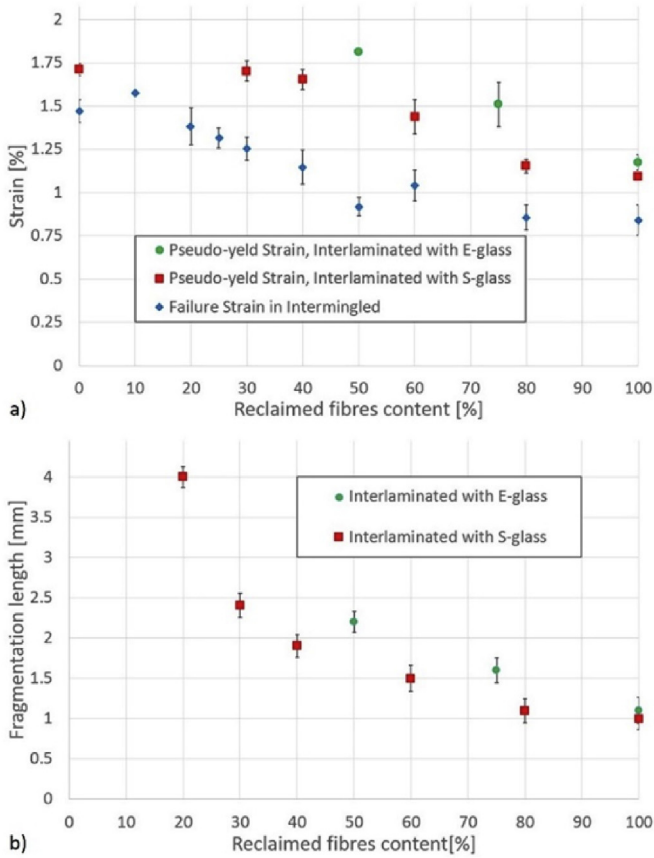
**Fig. 9.** Fragmentation behaviour of interlaminated specimens as function of the rCF content: a) Comparison with intermingled specimens; b) Fragmentation length.

vCF ratio on the failure mechanism. The absolute thickness of the rCF/vCF layer is represented on the vertical axis for a fixed total glass thickness, in this case 0.39 mm for E-glass, 0.49 mm for S-glass. Such Damage Mode Maps can help to find the optimum combination of ratios of the recycled to virgin CF content and the absolute thickness of the rCF/vCF layer embedded between glass/epoxy layers with a pre-known thickness.

Similar to the method presented in Ref. [34], the boundaries between different damage process zones are found by equating pairs of required stress for different failure modes of (i) high strain material failure, (ii) low strain material fragmentation and (iii) delamination. The only difference between the Damage Mode Maps in this paper and those in Refs. [34–36] is the parameters the maps are drawn for (x and y axes variable). More details about the map construction can be found in Refs. [34,36].

Fig. 10 shows the Damage Mode Map for reclaimed-virgin carbon interlaminated hybrid composites with E-glass and S-glass. The horizontal axis shows the failure strain of the rCF/vCF layer and the registered failure value for each set of specimen is shown on the graph. These values are slightly higher than those tested with end-tabs and without any outer glass layer shown in Fig. 5b because of stress concentration elimination around the end tabs, which is extensively discussed in Ref. [32]. For rCF content of 50%, 75% and 100% the damage initiation strains coincide with the pseudo-yield strains shown in Fig. 8b, and for 25% rCF, which failed suddenly, the damage initiation strain coincides with the specimen failure strain.

The Damage Mode Map explains the observed change in the failure process of the tested samples from catastrophic E-glass layer failure to carbon layer fragmentation. Increasing the rCF/vCF ratio

reduces the failure strain of the low strain material and results in specimen configurations in the fragmentation region. In the 25% rCF content specimen, the fracture of the discontinuous carbon fibre layer, i.e. the low strain material, causes failure of the continuous E-glass layer, as shown in Fig. 7a. In the case of the 75% and 100% rCF content specimens, the discontinuous carbon fibre layer fragmentation, starting at a lower level of strain, allows diffuse carbon fragmentation, as shown in Fig. 7a. Of particular interest is the case of the 50% rCF that falls very close to the boundary line between the carbon fragmentation and the glass failure regions in the Damage Mode Map of Fig. 10a and shows fragmentation and glass failure in Fig. 7a. This set of specimens with 50% rCF shows a high variation in its behaviour, as demonstrated by Fig. 11: Specimen 1 shows a pseudo-ductile behaviour as shown in Fig. 7a while Specimen 2 fails in a brittle manner. In other words, being close to the border lines means that with a slight material or geometry variability, the failure mode may switch to a different one.

Because of the higher strength of the S-glass, the predicted failure process for all tested samples with S-glass is carbon fragmentation followed by dispersed delamination, as shown in Fig. 10b. However, specimens with high ratios of vCF are closer to the boundary of the single carbon fracture followed by catastrophic delamination region. The effects of approaching the boundary line between "carbon fragmentation & delamination" and "carbon failure & catastrophic delamination" appear evident in Fig. 9b: the number of fragments is reduced and the delaminated area
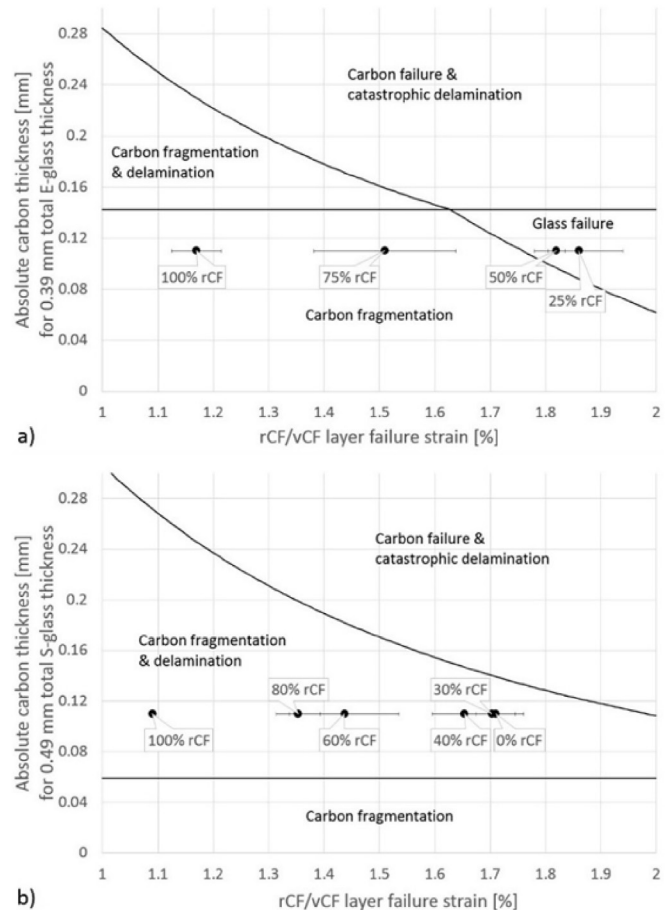


**Fig. 10.** Damage Mode Map for interlaminated hybrid composites: a) With E-glass; b) With S-glass.
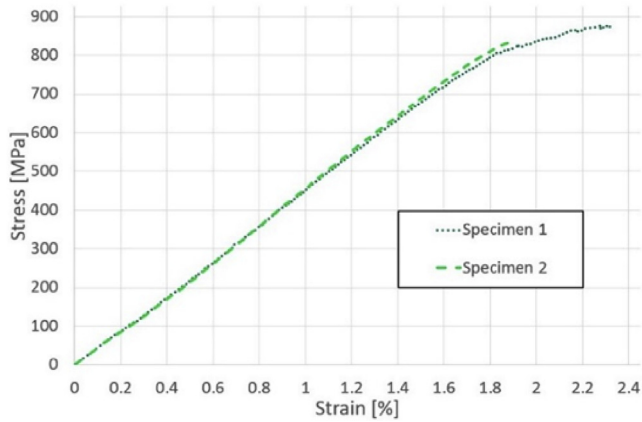
**Fig. 11.** 50% rCF specimens with pseudo-ductile and elastic-brittle behaviour.

increases.

By changing the carbon/glass thickness ratio and also the rCF/vCF ratios, it is possible to increase the hybrid composite stiffness and optimise the shape of the stress-strain curve to maximise the pseudo-ductile response. Fig. 12 shows the potential stiffness and pseudo-ductile strain values and the optimum failure strain and absolute thickness of the rCF/vCR carbon layer. In particular, observing the Damage Mode Map for the interlaminated hybrids with E-glass (Fig. 12a), it can be concluded that by using contents of rCF over 75% i.e. a rCF/vCF layer failure strain of less than 1.5%, and an absolute carbon thickness of more than 0.15 it is possible to move into the region of carbon fragmentation and delamination, increasing the total stiffness and the pseudo-ductile strain. For both the S-glass and the E-glass cases the higher the content of rCF the higher the possibility to increase the stiffness by increasing the carbon layer thickness and at the same time maximise the pseudo-ductile strain.

## 5. Conclusion

This paper demonstrates that not only is it possible to remanufacture reclaimed carbon fibre into high mechanical properties recycled composite materials with high mechanical properties, but also to use rCF to modulate the pseudo-ductile response of interlaminated hybrid composites.

The failure behaviour of intermingled rCF-vCF composites can be explained using the linear and bilinear rule of mixtures
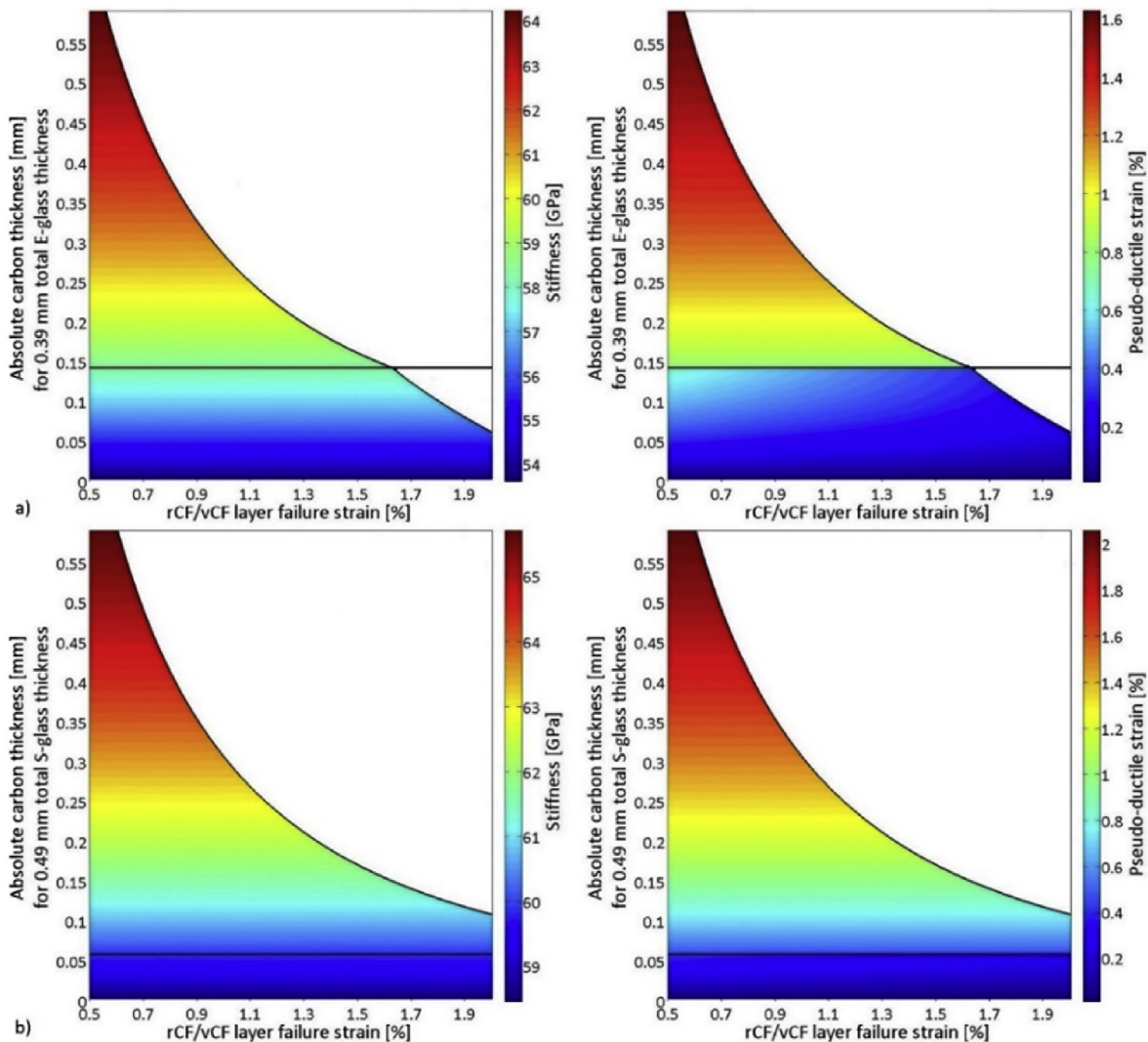


**Fig. 12.** Damage mode maps with stiffness and pseudo-ductile strain variation for interlaminated hybrid composites: a) With E-glass; b) With S-glass.

envelope. As expected, the fibre strength reduction caused by the reclamation process is reflected by a decay in the failure strain and strength of the composite material. On one hand, this can be accepted if the loss in strength is compensated by the economic benefits of using a cheaper raw material, on the other hand, the constant development of the reclaiming techniques is delivering reclaimed fibres with a minimal loss of strength, making recycled composites a viable solution for high performance applications.

When intermingled rCF/vCF are coupled with continuous glass fibre to create interlaminated composites, a pseudo-ductile behaviour has been obtained. Different ratios of rCF in the intermingled layer led to variation in the failure mechanism and in the stress-strain curve characteristics, i.e. the pseudo-yield point and pseudo-ductile strain. The Damage Mode Maps can describe this behaviour quite well, and will be a valuable tool to optimise the design of the materials. For example the rCV/vCF content ratio in the intermingled layer and the Carbon/Glass thickness ratio can be selected to obtain specific values of stiffness and pseudo-yield strain. This needs to be verified with further experimental investigation.

Finally, the HiPerDiF method proved to be an extremely valuable technique to generate hierarchically organised pseudo-ductile composites with discontinuous fibres and an efficient platform to remanufacture reclaimed carbon fibres into a recycled composite material with high mechanical properties and economical value.

## Acknowledgments

All necessary data to support the conclusions are provided in the results section of this paper.

## References

[1] S. Pimenta, S.T. Pinho, Recycling carbon fibre reinforced polymers for structural applications: technology review and market outlook, Waste Manag. 31 (2011) 378—392.

[2] L.O. Meyer, K. Schulte, E. Grove-Nielsen, CFRP-recycling following a pyrolysis route: process optimisation and potentials, J. Compos. Mater. 43 (9) (2009) 1121—1132.

[3] S.J. Pickering, R.M. Kelly, J.R. Kennerley, C.D. Rudd, N.J. Fenwick, A fluidised bed process for the recovery of glass fibres from scrap thermoset composites, Compos. Sci. Technol. 60 (2000) 509—523.

[4] R.E. Allred, J.M. Gosau, J.M. Shoemaker, Recycling process for carbon/epoxy composites, in: SAMPE 2001 Symposium & Exhibition, SAMPE, 2001. Longbeach, CA, USA.

[5] M. Nakagawa, K. Shibata, H. Kuriya, Characterization of CFRP using recovered carbon fibers from waste CFRP, in: Second International Symposium on Fiber Recycling, the Fiber Recycling 2009 Organizing Committee, 2009. Atlanta, Georgia, USA.

[6] R. Pinero-Hernanz, C. Dodds, J. Hyde, J. Garcia-Serna, M. Poliakoff, E. Lester, M.J. Cocero, S. Kingman, S.J. Pickering, K.H. Wong, Chemical recycling of carbon fibre reinforced composites in nearcritical and supercritical water, Compos. Part A Appl. Sci. Manuf. 39 (2008) 454—461.

[7] R. Pinero-Hernanz, J. Garcia-Serna, C. Dodds, J. Hyde, M. Poliakoff, M.J. Cocero, S. Kingman, S.J. Pickering, E. Lester, Chemical recycling of carbon fibre composites using alcohols under subcritical and supercritical conditions, J. Supercrit. Fluids 46 (2008) 83—92.

[8] G. Jiang, S.J. Pickering, E.H. Lester, T.A. Turner, K.H. Wong, N.A. Warrior, Characterisation of carbon fibres recycled from carbon fibre/epoxy resin composites using supercritical n-propanol, Compos. Sci. Technol. 69 (2009) 192—198.

[9] M. Goto, Chemical recycling of plastics using sub- and supercritical fluids, J. Supercrit. Fluids 47 (2009) 500—507.

[10] J. Meredith, S. Cozien-Cazucb, E. Collings, S. Carter, S. Alsopd, J. Levera, S.R. Colesa, B.M. Wood, K. Kirwan, Recycled carbon fibre for high performance energy absorption, Compos. Sci. Technol. 72 (2012) 668—695.

[11] K.H. Wong, S.J. Pickering, T.A. Turner, N.A. Warrior, Compression moulding of a recycled carbon fibre reinforced epoxy composite, in: SAMPE'09 Conference, SAMPE, 2009. Baltimore, MD, USA.

[12] S.J. Pickering, Recycling technologies for thermoset composite materials - current status, Compos. Part A Appl. Sci. Manuf. 37 (2006) 1206—1215.

[13] M. Szpieg, M. Wysocki, L.E. Asp, Reuse of polymer materials and carbon fibres in novel engineering composite materials, Plastics, Rubber Compos. 38 (2009) 419—425.

[14] T.A. Turner, S.J. Pickering, N.A. Warrior, Development of high value composite materials using recycled carbon fibre, in: SAMPE'09 Conference, SAMPE, 2009. Baltimore, MD, USA.

[15] L.T. Harper, T.A. Turner, J.R.B. Martin, N.A. Warrior, Fibre alignment in directed carbon fibre preforms-a feasibility test, J. Compos. Mater. 43 (1) (2009) 57—74.

[16] K.H. Wong, T.A. Turner, S.J. Pickering, N.A. Warrior, The potential for fibre alignment in the manufacture of polymer composites from recycled carbon fibre, SAE Int. J. Aero space 2 (1) (2009) 225—231.

[17] S.J. Pickering, Carbon fibre recycling technologies: what goes in and what comes out?, in: Carbon Fibre Recycling and Reuse 2009 Conference, Inter-techPira, Hamburg, Germany, 2009.

[18] K.H. Wong, S.J. Pickering, C.D. Rudd, Recycled carbon fibre reinforced polymer composite for electromagnetic interference shielding, Compos. Part A Appl. Sci. Manuf. 41 (2010) 693—702.

[19] K.H. Wong, T.A. Turner, S.J. Pickering, N.A. Warrior, The potential for fibre alignment in the manufacture of polymer composites from recycled carbon fibre, in: SAE AeroTech Congress and Exhibition, SAE International, Seattle, Washington, USA, 2009.

[20] M.E.G. Janney Jr., N. Baitcher, Fabrication of chopped fiber preforms by the 3-DEP process, in: Composites and Polycon 2007, American Composites Manufactureres Association, Tampa, FL, USA, 2007.

[21] H. Yu, K.D. Potter, "Method and apparatus for aligning discontinuous fibres" UK patent, Patent application number 1306762.4, 2013.

[22] H. Yu, K.D. Potter, M.R. Wisnom, A novel manufacturing method for aligned discontinuous fibre composites (High Performance-Discontinuous Fibre Method), Compos. Part A Appl. Sci. Manuf. 65 (2014) 175—185.

[23] H. Yu, M.L. Longana, M. Jalalvand, M.R. Wisnom, K.D. Potter, Pseudo-ductility in intermingled carbon/glass hybrid composites with highly aligned discontinuous fibres, Compos. Part A Appl. Sci. Manuf. 73 (2015) 35—44.

[24] H. Yu, M.L. Longana, M. Jalalvand, M.R. Wisnom, K.D. Potter, Hierarchical Pseudo-ductile Hybrid Composites with Continuous and Highly Aligned Discontinuous Fibres, 2017. ARTICLE IN PRESS.

[25] M.L. Longana, N. Ong, H. Yu, K.D. Potter, Multiple closed loop recycling of carbon fibre composites with the HiPerDiF (High Performance Discontinuous Fibre) method, Compos. Struct. 153 (2016) 271—277.

[26] http://www.tohotenax.com/products/tenax%C2%AE-carbon-fiber/tenax%C2%AE-short-fibers and personal correspondence.

[27] S. Pimenta, S.T. Pinho, The effect of recycling on the mechanical response of carbon fibres and their composites, Compos. Struct. 94 (12) (2012) 3669—3684.

[28] https://cytec.com/sites/default/files/datasheets/MTM49.pdf.

[29] J. Aveston, G.A. Cooper, A. Kelly, Single and multiple fracture, in: The Properties of Fibre Composites: Conference Proceedings, National Physical Laboratories, UK, 1971.

[30] G. Kretsis, A review of the tensile, compressive, flexural and shear properties of hybrid fibre-reinforced plastics, Composites 18 (1) (1987) 13—23.

[31] M.R. Wisnom, Mechanisms to create high performance pseudo-ductile composites, in: IOP Conference Series: Materials Science and Engineering 139, 37th Risø International Symposium on Materials Science, September 2016.

[32] G. Czél, M. Jalalvand, M.R. Wisnom, Hybrid Specimens Eliminating Stress Concentrations in Tensile and Compressive Testing of Unidirectional Composites, 2017. ARTICLE IN PRESS.

[33] Ha. Yu, M.L. Longana, Y. Swolfs, M.R. Wisnom, K.D. Potter, Hybrid effect of carbon/glass composites as a function of the strength distribution of aligned short carbon fibres, in: Proceedings of ECCM17, 26—30th June 2016. Munich, Germany.

[34] M. Jalalvand, G. Czél, M.R. Wisnom, Numerical modelling of the damage modes in UD thin carbon/glass hybrid laminates, Compos. Sci. Technol. 94 (2014) 39—47.

[35] M. Jalalvand, G. Czél, M.R. Wisnom, Parametric study of failure mechanisms and optimal configurations of pseudo-ductile thin-ply UD hybrid composites, Compos. Part A Appl. Sci. Manuf. 74 (2015) 123—131.

[36] M. Jalalvand, G. Czél, M.R. Wisnom, Damage analysis of pseudo-ductile thin-ply UD hybrid composites - a new analytical method, Compos. Part A Appl. Sci. Manuf. 69 (2015) 83—93.